Redox Biology 45 (2021) 102045

Contents lists available at ScienceDirect

Redox Biology

journal homepage: www.elsevier.com/locate/redox

A new thiol-independent mechanism of epithelial host defense against *Pseudomonas aeruginosa*: iNOS/NO• sabotage of theft-ferroptosis

Haider H. Dar [a,*], Tamil S. Anthonymuthu [b], Liubov A. Ponomareva [c], Austin B. Souryavong [a], Galina V. Shurin [a], Alexandr O. Kapralov [a], Vladimir A. Tyurin [a], Janet S. Lee [d], Rama K. Mallampalli [e], Sally E. Wenzel [a,f], Hülya Bayir [a,b,**], Valerian E. Kagan [a,c,g,***]

[a] Department of Environmental and Occupational Health and Center for Free Radical and Antioxidant Health, University of Pittsburgh, Pittsburgh, PA, USA
[b] Department of Critical Care Medicine, Safar Center for Resuscitation Research, Children's Neuroscience Institute, Children's Hospital of Pittsburgh, University of Pittsburgh, Pittsburgh, PA, USA
[c] Institute for Regenerative Medicine, IM Sechenov Moscow State Medical University, Moscow, Russia
[d] Department of Medicine, Division of Pulmonary, Allergy, Critical Care Medicine, Acute Lung Injury Center of Excellence, University of Pittsburgh, Pittsburgh, PA, USA
[e] Department of Internal Medicine, The Ohio State University, Columbus, OH, USA
[f] Asthma Institute, University of Pittsburgh, PA, USA
[g] Departments of Pharmacology and Chemical Biology, Chemistry, Radiation Oncology, University of Pittsburgh, PA, USA

ARTICLE INFO

Keywords:
Lipid peroxidation
GPx4
Degradation
Theft-ferroptosis
iNOS/nitric
Oxide
Pseudomonas aeruginosa

ABSTRACT

Ferroptosis is a redox-driven type of regulated cell death program arising from maladaptation of three metabolic pathways: glutathione homeostasis, iron handling and lipid peroxidation. Though GSH/Gpx4 is the predominant system detoxifying phospholipid hydroperoxides (PLOOH) in mammalian cells, recently Gpx4-independent regulators of ferroptosis like ferroptosis suppressor protein 1 (FSP1) in resistant cancer lines and iNOS/NO• in M1 macrophages have been discovered. We previously reported that *Pseudomonas aeruginosa* (PA) utilizes its 15-lipoxygenase (pLoxA) to trigger ferroptotic death in epithelial cells by oxidizing the host arachidonoyl-phosphatidylethanolamine (ETE-PE) into pro-ferroptotic 15-hydroperoxy- arachidonyl-PE (15-HpETE-PE). Here we demonstrate that PA degrades the host GPx4 defense by activating the lysosomal chaperone-mediated autophagy (CMA). In response, the host stimulates the iNOS/NO•-driven anti-ferroptotic mechanism to stymie lipid peroxidation and protect GPx4/GSH-deficient cells. By using a co-culture model system, we showed that macrophage-produced NO• can distantly prevent PA stimulated ferroptosis in epithelial cells as an inter-cellular mechanism. We further established that suppression of ferroptosis in epithelial cells by NO• is enabled through the suppression of phospholipid peroxidation, particularly the production of pro-ferroptotic 15-HpETE-PE signals. Pharmacological targeting of iNOS (NO• generation) attenuated its anti-ferroptotic function. In conclusion, our findings define a new inter-cellular ferroptosis suppression mechanism which may represent a new strategy of the host against *P. aeruginosa* induced theft-ferroptosis.

1. Introduction

Upon infection, host cells and bacteria enter a tug-of-war [1] in which the invader attempts to make the host environment more favorable to survival and dissemination, whereas the host cells try to mount an effective defense [1,2]. Multiple mechanisms aimed at dampening the host response, including hijacking of mammalian programs of regulated cell death, are enacted by bacteria [3]. Commonly, a number of cell death programs - apoptosis, pyroptosis, necroptosis, autophagic cell death - are employed by the host to counteract the infection [4–6]. However, these same programs may be manipulated and used by pathogens to reverse the role of the cell death process and its outcome in

* Corresponding author.
** Corresponding author. Department of Environmental and Occupational Health and Center for Free Radical and Antioxidant Health University of Pittsburgh, Pittsburgh, PA, USA.
*** Corresponding author. Department of Environmental and Occupational Health and Center for Free Radical and Antioxidant Health University of Pittsburgh, Pittsburgh, PA, USA.
E-mail addresses: had39@pitt.edu (H.H. Dar), bayihx@ccm.upmc.edu (H. Bayir), kagan@pitt.edu (V.E. Kagan).

https://doi.org/10.1016/j.redox.2021.102045
Received 24 March 2021; Received in revised form 4 May 2021; Accepted 11 June 2021
Available online 16 June 2021

their favor [7–9]. One of the latest examples of this is the use of a newly discovered regulated cell death (RCD) program, ferroptosis, by an opportunistic Gram-negative bacterium *Pseudomonas aeruginosa* [10].

In mammalian cells, ferroptosis is triggered by the imbalanced synchronization of iron, thiols and lipids resulting in the selective peroxidation of arachidonoyl-PE (ETE-PE) into pro-ferroptotic 15-hydroperoxy-arachidonyl-PE (15-HpETE-PE) [11–14]. One of the likely catalysts of this reaction is 15- lipoxygenase (15LOX) complexed with a scaffold protein, PE-binding protein-1 (PEBP1) [15–17]. Ferroptosis has also been reported to play a pathogenic role in bacterial infection induced host cell damage [10,18]. We described that *P. aeruginosa* (PA) exploits "theft-ferroptosis" as a virulence mechanism utilizing a specialized 15LOX, pLOXA [10]. This is achieved by targeting and hijacking the host redox lipid remodeling pathway leading to the accumulation of proferroptotic phospholipid hydroperoxides in human bronchial epithelial cells [10]. To counter, host cells usually employ a unique selenoenzyme from the glutathione peroxidase family, GPx4, that specifically reduces phospholipid hydroperoxides to the respective non-ferroptotic alcohols [19,20]. In addition to this main "watchdog" of ferroptotic cell death, recent studies have identified several new GPx4 independent regulators of ferroptosis, explaining the resistance mechanisms exhibited by some cell types [21–24]. In this context, we demonstrated that among the host immune cells, macrophages in M1 activation state expressing iNOS/NO• are resistant to ferroptosis [23].

NO• is a reactive molecule produced by nitric oxide synthase (NOS) family of proteins. NO• directly binds and inactivates Fe-containing enzymes [25,26] or reacts with superoxide anion-radical O2• - to form a highly reactive peroxynitrite (OONO-) attacking pathogen's

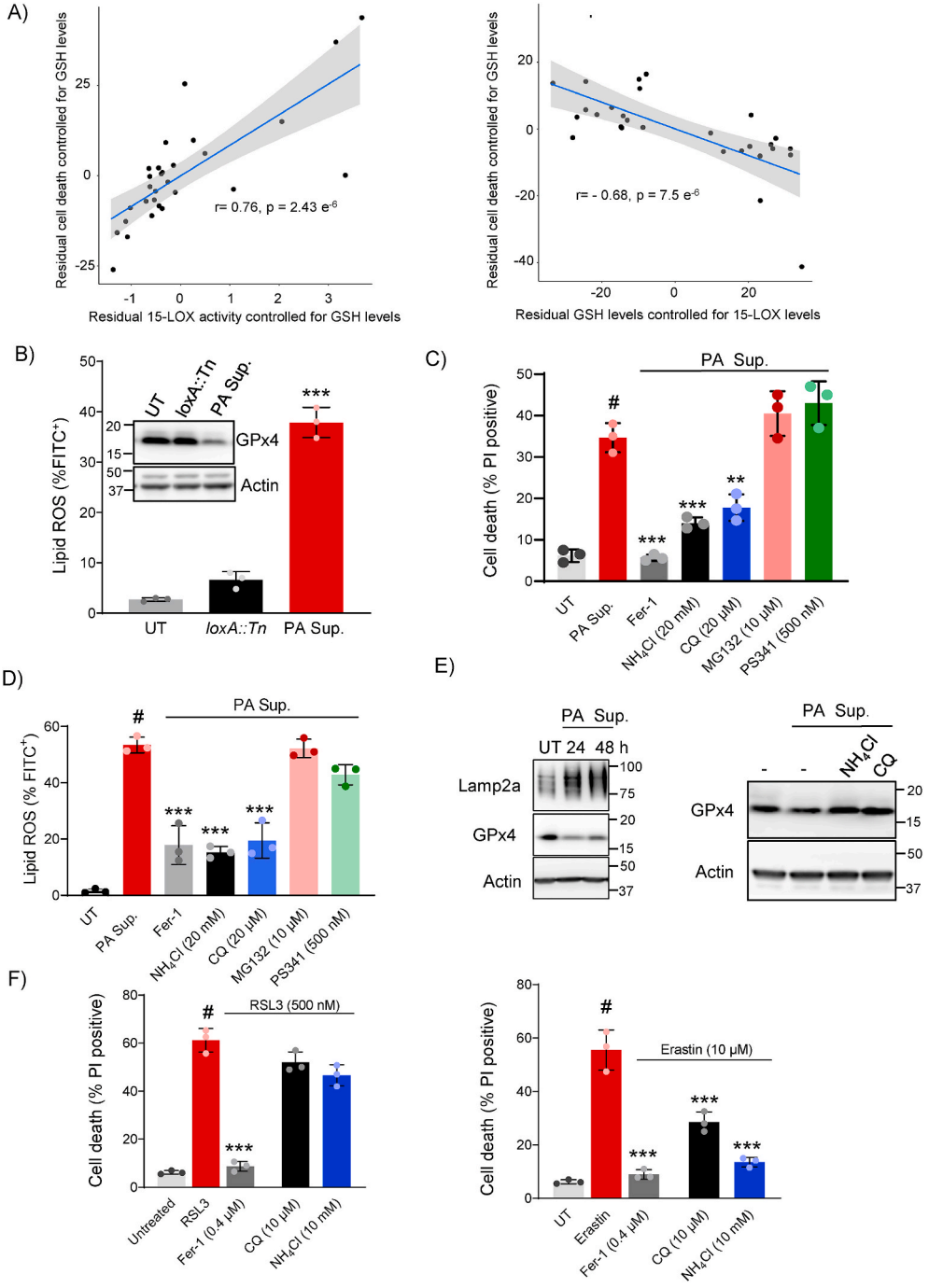

Fig. 1. PA degrades host GPx4 through activation of the chaperone-mediated autophagy (CMA) pathway. (**A**) Partial correlation analysis between pLoxA activity and ferroptotic death of host (epithelial cells) controlled for GSH levels after treatment with PA (**left panel**) or between residual GSH levels controlled for pLoxA activity and ferroptotic cell death after treatment with PA (**right panel**). Each dot represents individual clinical isolate. (**B**) Lipid ROS levels measured in epithelial cells (HBE) after treatment with PA supernatant with or without pLoxA using BODIPY. Inset: Western blot demonstrating decrease in GPx4 expression after treatment with pLoxA containing supernatant. ***p < 0.0001 relative to UT (untreated) or *loxA::Tn* (n = 3). (**C** & **D**) Epithelial cells were treated with PA Sup. in the presence of indicated inhibitors. Cell death or Lipid ROS was estimated by PI or BODIPY staining and analyzed by flow cytometry. #p < 0.0001 relative to UT (untreated); ***p < 0.0001; **p < 0.001 relative to PA Sup. (n = 3). (**E**) Western blot showing decreased expression of GPx4 and activation of Lamp2a in epithelial cells after treatment with PA supernatant (**left panel**) and rescue of GPx4 in presence of NH_4Cl or Chloroquine (CQ) (**right panel**). (**F**) Epithelial cells were treated with RSL3 (500 nM) or erastin (10 μM) along with different inhibitors of protein degradation pathways. Cell death monitored by PI staining using flow cytometry. #p < 0.0001 relative to UT (untreated); ***p < 0.0001 relative to RSL3 or erastin. (n = 3).

membrane lipids and proteins, particularly protein thiols [27,28]. In this way, $NO^{\bullet}$ exerts bactericidal and bacteriostatic propensities within macrophages acting as an essential part of the host defense against pathogens [29].

Similar to other types of regulated cell death, ferroptosis uses intrinsic cellular machinery for the program execution. However, quite distinctively, ferroptosis is a non-cell autonomous program, that can spread and impact the neighboring cells [30,31]. Given the diffusible signaling characteristics of $NO^{\bullet}$ and its ability to protect M1 macrophages from ferroptosis, we envisioned a unique intercellular anti-ferroptotic protection by $NO^{\bullet}$, particularly in the context of host-pathogen interactions. Here, using a two-cell epithelial and macrophage coculture system, we demonstrate that i) PA targets host GPx4/GSH system prompting degradation of GPx4 and promoting ferroptosis; ii) PA-stimulated macrophages generate $NO^{\bullet}$ which prevents phospholipid peroxidation, particularly the production of pro-ferroptotic 15- HpETE-PE signals, and hence protecting against ferroptosis in macrophages as well as in neighboring epithelial cells; iii) using si-RNA mediated knock-down (KD) approach in epithelial cells, we validated that even under GPx4 insufficient conditions, iNOS/$NO^{\bullet}$ protects cells against ferroptosis.

2. Results

2.1. PA targets host GPx4/GSH system

PA produces, secretes and utilizes outer membrane vesicles (OMVs) as virulence factors which interact and alter host cell biology [32–34]. Among them are inducers of ferroptosis, including pLoxA [10]. We previously observed that pLoxA activity of the pathogen OMV (supernatants) and the GSH levels of host cells collectively are promising predictors of ferroptotic cell death [10]. However, to assess their individual contributions and to understand whether the changes induced by the pathogen and host responses are dependent on one another, we performed partial correlation analysis between pLoxA activity of *P. aeruginosa* clinical isolates and ferroptosis while controlling for host GSH levels (Fig. 1A, **left panel**). Conversely, controlling for pLoxA activity, we performed partial correlation analysis of host GSH levels after treatment with *P. aeruginosa* clinical isolates and cell death (Fig. 1A, **right panel**). At constant GSH levels in host cells, the pLoxA activity elicits a robust positive correlation with cell death (r value of 0.76, $p = 2.4 \times 10^{-6}$). Similarly, maintaining pLoxA activity of the supernatants constant, the host GSH levels displayed a strong negative correlation with cell death (r value of - 0.68 and $p = 7.5 \times 10^{-5}$), (Fig. 1A, **right panel**). This suggests that the two factors, pLoxA activity of the pathogen and the GSH levels of host, are independent of each other; however, collectively they produce a synergistic effect. It also implies that for proficient theft-ferroptosis to occur, PA supernatant in addition to containing the pLoxA also targets the GPx4/GSH defense system of the host.

GSH-dependent selenoenzyme GPx4 is a central anti-ferroptotic defense system of the host that controls ferroptosis by reducing the pro-ferroptotic signal 15-HpETE-PE to non-ferroptotic 15- hydroxy-arachidonoyl-phosphatidylethanolmine (15-HETE-PE) [12,20,35]. Sufficiency of this system maintains cellular homeostasis and resistance to ferroptotic death program [20]. We found that treatment with pLoxA-containing supernatant targeted GPx4 and degraded it in a pLoxA dependent manner (Fig. 1B). Treatment with PA supernatant was also accompanied by a significant decrease in the activity of GPx4 (Supplementary Fig. 1A). Expectedly, the treatment caused enhanced "lipid ROS" as indicated by BODIPY oxidation (Fig. 1B). In contrast, the supernatant from pLoxA deficient mutant (*loxA::Tn*) was not able to affect either the GPx4 protein levels or induce lipid peroxidation (Fig. 1B).

2.2. PA activates host CMA pathway for the degradation of GPx4

Host protein regulatory pathways are one of the major targets of pathogens. It has been reported that *P. aeruginosa* exploits the host ubiquitination signaling pathways for its successful progression [36]. Therefore, we next explored the host protein degradation pathway targeted by PA supernatant to manipulate the GPx4 protein levels. For this we incubated HBE cells with PA supernatant and commonly used inhibitors of proteasomal (MG132 and PS341) or lysosomal (NH_4Cl and Chloroquine) degradation pathways (Fig. 1C). Only NH_4Cl and Chloroquine (CQ) displayed significant inhibition of ferroptosis suggesting the involvement of lysosomal pathway in GPx4 degradation (Fig. 1C). Both NH_4Cl and CQ also inhibited lipid ROS, while the proteasomal inhibitors (MG132 and PS341) were inept in protecting epithelial cells from BODIPY oxidation (Fig. 1D). Further, we confirmed the involvement of lysosomal degradation pathway by testing activation of Lamp2a after treatment with PA supernatant and found that the Lamp2a levels were considerably increased (Fig. 1E, **left panel**). Lamp2a is a hallmark for CMA-a specific lysosomal protein degradation pathway [37,38]. Notably, the decrease in levels of GPx4 protein by PA treatment were rescued by both NH_4Cl and CQ (Fig. 1E, **right panel**).

There are several types of ferroptosis inducers [39,40]. Two of them affect either the pathways controlling GSH levels (e.g., erastin inhibiting cystine/glutamate antiporter) [39,41] or GPx4 activity (e.g., RSL3, ML162). Our results indicate that CMA-inhibitors, NH_4Cl and CQ, rescued cells from erastin induced ferroptotic death but not from RSL3 induced ferroptosis (Fig. 1F). None of the inhibitors affected erastin dependent decrease in GSH/GSSG (Supplementary Fig. 1B). Based upon these findings, we conclude that co-incubation of epithelial cells with PA supernatant leads to inactivation of the "host" GPx4/GSH defense system yielding ferroptosis.

2.3. iNOS/$NO^{\bullet}$ rescues epithelial cells from PA induced ferroptotic cell death

Pulmonary epithelial cells are surrounded by host immune cells such as macrophages whose job is to remove microbial threats. In the context of ferroptosis, macrophages are of particular importance since iNOS makes them resistant to ferroptosis [23]. Interestingly, incubation of macrophages with PA supernatant led to their transition to M1 phenotype with high level of iNOS expression (Fig. 2A) and resulting in resistance to ferroptosis (Fig. 2B). Counting the amounts of macrophages after PA treatment revealed no difference in the cell numbers after activation (Supplementary Fig. 2A, left panel). Based on these findings, we explored whether expression of iNOS in macrophages may be sufficient to prevent the epithelium from PA induced ferroptosis. When epithelial cells were co-incubated with PA supernatant in the presence of macrophages, the ferroptotic death of epithelial cells was significantly suppressed (Fig. 2C). Since lipid peroxidation is a requirement for ferroptosis, we used BODIPY oxidation as an indicator of lipid peroxidation in our co-culture experiment and found that macrophages significantly blunted the generation of lipid peroxidation in epithelial cells (Fig. 2D).

2.4. Epithelial cells and iNOS

iNOS can also be expressed by epithelial cells in response to cytokines or bacterial products [26,42]. Therefore, we examined the levels of iNOS in HBE cells incubated in the presence of PA supernatant. Treatment with PA supernatant did not stimulate the expression of iNOS in these cells (Fig. 2E). Next, we wanted to know whether iNOS/$NO^{\bullet}$ can function as anti-ferroptotic regulator in epithelial cells. For this, we expressed iNOS in epithelial cells and then treated them with PA supernatant or RSL3 or erastin to trigger ferroptosis. Indeed, we found that iNOS expressing epithelial cells were resistant not only to PA supernatant initiated ferroptotic insult but also to other commonly used ferroptosis inducers like RSL3 and erastin (Fig. 2F and G). Expression of

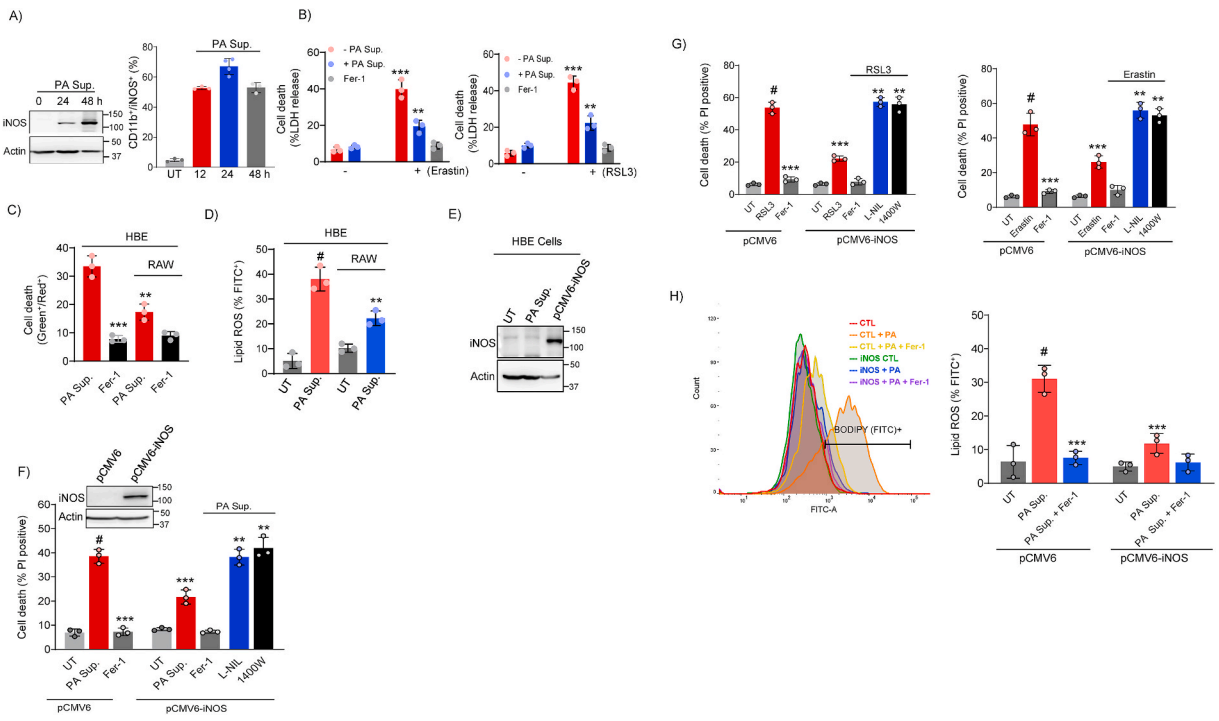

Fig. 2. iNOS/NO• protects epithelial cells from ferroptosis. (**A**) Expression of iNOS in macrophages after treatment with PA supernatant by western blotting (**left panel**) and by flow cytometry (**right panel**) (n = 3). (**B**) Macrophages were activated with PA supernatant for 24 h and then treated with erastin (**left panel**) or RSL3 (**right panel**) along with ferrostatin 1 (Fer-1, 0.4 μM). Cell death was measured by LDH release assay after 14 h. ***p < 0.0001 relative to samples without (erasin/RSL3), **p < 0.001 vs RSL3 or erastin alone (n = 3). (**C** & **D**) Epithelial cells were co-cultured with macrophages (1:1) in 6 well plates and then treated with PA supernatant. Cell death and Lipid ROS was measured by Zombie staining and BODIPY using the flow cytometry. ***p < 0.0001; **p < 0.001 relative to HBE + PA Sup.; #p < 0.0001 vs UT (untreated HBE only). (n = 3). (**E**) Expression of iNOS in epithelial cells after PA treatment. (**F** & **G**) Epithelial cells were transfected with vector only (pCMV6) or with iNOS (pCMV6-iNOS) and then treated with PA supernatant (**F**) or with RSL3 (500 nM) or erastin (10 μM) (**G**) in the absence or presence Fer-1 or iNOS inhibitors. #p < 0.0001 vs UT (untreated); ***p < 0.0001 relative to PA Sup./RSL3/erastin; **p < 0.001 vs pCMV6-iNOS treated PA Sup./RSL3/erastin. (n = 3). (**H**) Epithelial cells with or without iNOS were treated with PA Sup. Lipid ROS was determined by BODIPY staining and analyzed by flow cytometry. #p < 0.0001 vs UT; ***p < 0.0001 relative to PA Sup. without iNOS. (n = 3).

iNOS did not increase epithelial cell proliferation (Supplementary Fig. 2A, right panel). To confirm that the protection was due to iNOS/NO•, we used specific inhibitors (L-NIL and 1400W) of NO• generation, which abolished iNOS/NO• mediated protection against ferroptotic death of epithelial cells (Fig. 2F and G). A similar protection against PA induced ferroptosis was observed in iNOS expressing HT-1080 cells and by the addition of NO-donors (Supplementary Figs. 2B and C). Furthermore, similar to GPx4 (Supplementary Fig. 2D), expression of iNOS led to a decreased lipid ROS production after PA treatment (Fig. 2H) thus supporting the GPx4-like effect of iNOS.

2.5. iNOS/NO• does not influence GPx4 protein levels

Given that functional GPx4/GSH system is sufficient in preventing ferroptosis, we examined the relationships between the two systems – thiols and iNOS/NO•. Specifically, we wanted to know whether iNOS/NO• can regulate GPx4 at the protein level. For this, we performed two sets of experiments; i) we tested the stability of GPx4 in the presence of iNOS in HBE cells and ii) PA induced degradation of GPx4. Expression of iNOS/NO• did not alter the stability of GPx4 under basal conditions or with PA supernatant stimulation (Fig. 3A). We also estimated GSH levels in vector or iNOS expressing HBE cells treated with erastin and found no significant differences (Fig. 3B). We further confirmed that iNOS induction in macrophages fails to stabilize GPx4 expression following stimulation with PA supernatant (Fig. 3C). These results emphasize that protection of PA induced ferroptosis by iNOS/NO• is not achieved through manipulation of GPx4/GSH system but through an independent mechanism.

2.6. iNOS/NO• induced protection is independent of GPx4

Next, we asked whether iNOS/NO• can protect epithelial cells from PA stimulated ferroptotic cell death under GPx4 limiting conditions. For this, we first knocked-down (KD) GPx4 using si-RNA and then expressed iNOS. KD was confirmed by western blotting (Fig. 3D, **left panel**). We observed that the decrease in the amount of GPx4 protein sensitized epithelial cells to PA induced ferroptosis and lipid ROS (Fig. 3D and E). Remarkably, expression of iNOS/NO• rescued GPx4-deficient cells from both lipid ROS and ferroptotic death (Fig. 3D and E).

2.7. Macrophage mediated protection is achieved via intercellular transfer of NO• from macrophages to epithelial cells

Under conditions of PA induced deficiency of GPx4/GSH anti-ferroptotic defense in host epithelial cells, the potential of iNOS/NO• to act remotely and independently of GPx4 bestows the host with a unique intercellular mechanism to protect the epithelial cells from PA. To examine this role of NO•, we performed a co-culture experiment in the presence of specific inhibitor of iNOS, which significantly eliminated the protection of epithelial cells and made them sensitive to PA induced ferroptosis (Fig. 4A). As a second line of evidence, we employed si-RNA to knock-down iNOS in macrophages and then used them for co-culture experiment. Again, we found that iNOS deficient macrophages were incompetent to rescue epithelial cells from PA supernatant induced ferroptotic cell death (Fig. 4B).

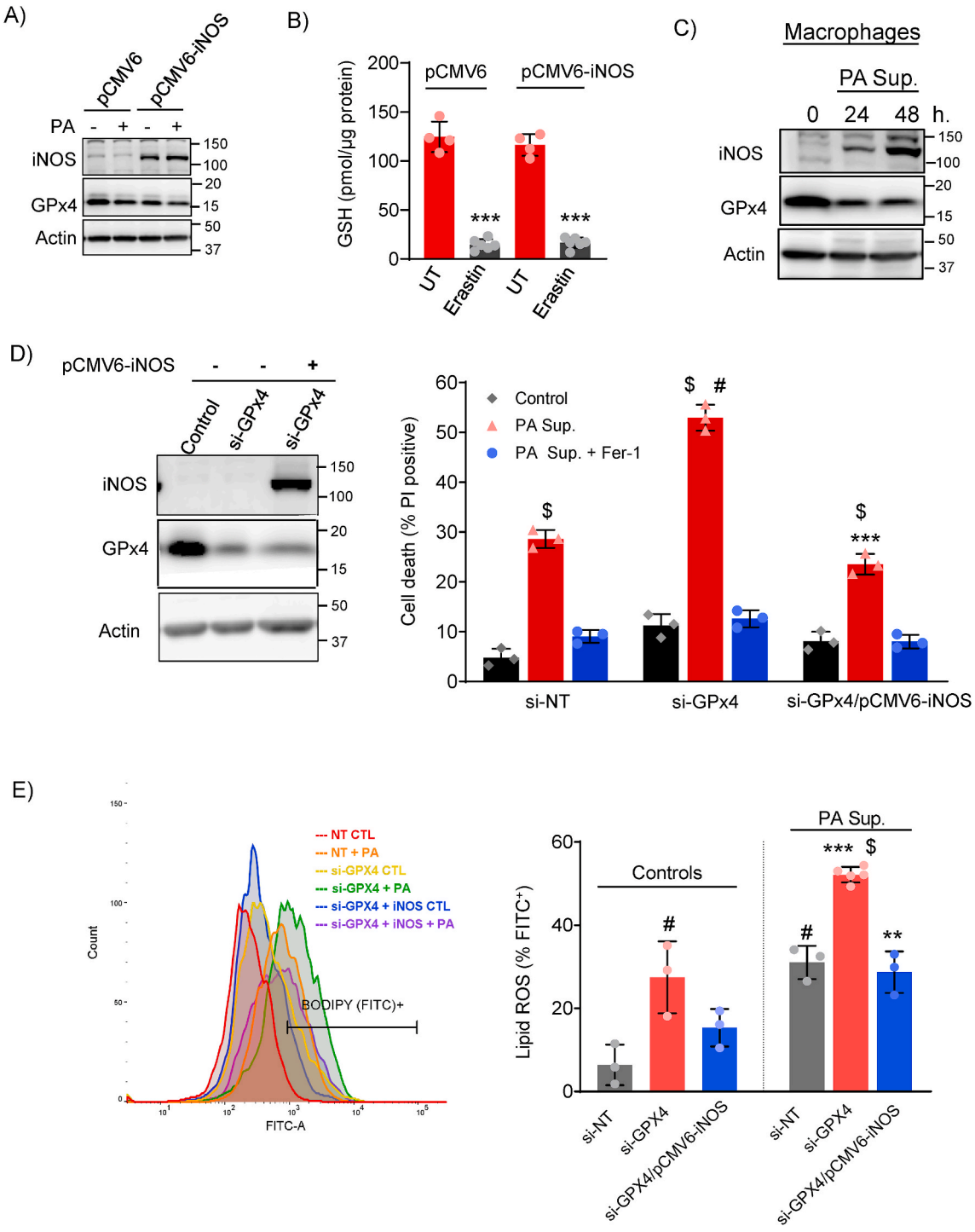

Fig. 3. iNOS/NO• mediated protection against ferroptosis does not influence GPx4 and is independent of GPx4. (**A** & **B**) Epithelial cells (HBE) with or without iNOS were treated with PA supernatant or erastin, then GPx4 protein (**A**) or GSH levels (**B**) was analyzed by western blotting or GSH assay respectively. ***$p < 0.0001$ UT (untreated). (n = 3–6). (**C**) Macrophages were treated with PA supernatant (PA Sup.) for different time points and then GPx4 and iNOS protein levels were examined by western blotting. (**D**) Ferroptosis protection by iNOS is independent of GPx4. Epithelial cells were transfected with si-GPx4 or si-NT (non-target) for 8 h and then with iNOS (pCMV6-iNOS) for 20 h. si-NT, GPx4 knock-down (KD) and GPx4 KD + iNOS cells were treated with PA supernatant along with Fer-1. $^{\$}p < 0.0001$ vs respective controls; $^{\#}p < 0.0001$ vs si-NT + PA Sup.; ***$p < 0.0001$ relative to si-GPx4 + PA Sup. **Left panel**, showing expression of GPx4 and iNOS, (n = 3). (**E**) Lipid ROS was measured by BODIPY staining and analyzed by flow cytometry in si-NT, si-Gpx4 and si-Gpx4 + iNOS treated with or without PA supernatant. $^{\#}p < 0.0001$ vs si-NT (control); $^{\$}p < 0.0001$ vs si-NT + PA Sup.; ***$p < 0.0001$ vs si-GPx4 (control); **$p < 0.001$ vs si-Gpx4 + PA Sup. (n = 3).

2.8. Redox phospholipidomics reveals reduction of proferroptotic signal (15-HpETE-PE) in epithelial cells cocultured with macrophages

Lipid peroxidation is the driver of ferroptotic cell death [12,43]. Since macrophage generated NO• does not regulate ferroptotic cell death at GPx4 level, we wondered whether NO• generated by macrophages could hinder the ferroptotic death signals. For this we labeled epithelial cells with Cell Tracker Green and co-cultured them with macrophages (1:1). After treatment with PA supernatant, we sorted epithelial cells by flow-cytometry and performed LC-MS redox

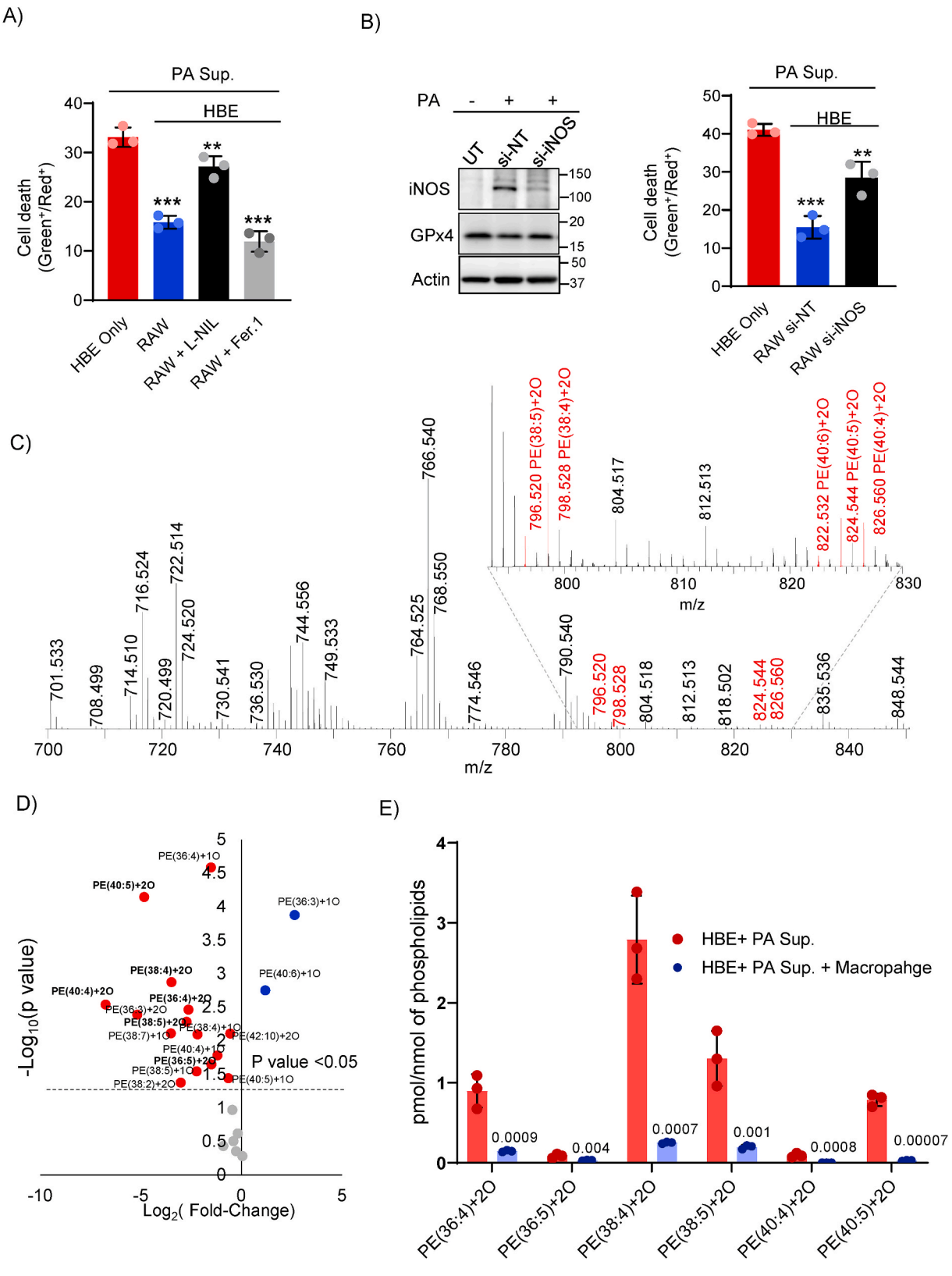

(caption on next page)

Fig. 4. Macrophage mediated protection is achieved via intercellular transfer of NO• from macrophages to epithelial cells. (**A**) Epithelial cells were labeled with Cell Tracker Green and then co-cultured with macrophages (1:1). Cells were then treated with PA Sup. along with iNOS inhibitor (L-NIL, 20 μM) or Fer-1 (0.4 μM). Cell death was analyzed by staining cells with Zombie dye using flow cytometry. Only double positive ($green^+/red^+$) cells were considered for analysis. ***p < 0.0001 vs HBE only + PA Sup., **p < 0.001 vs HBE + RAW + PA Sup. (n = 3). (**B**) Macrophages were transfected with control non-targeting si-RNA (si-NT) or si-iNOS and then co-cultured with Cell Tracker Green labeled epithelial cells. After treatment with PA supernatant, cell death was analyzed by flow cytometry. ***p < 0.0001 vs HBE only + PA Sup. **p < 0.001 vs HBE + RAW - si-NT + PA Sup. **Left panel** showing expression of iNOS, (n = 3). (**C**) Typical mass spectrum showing phosphatidyl ethanolamine extracted from epithelial cells. (**D**) Volcano plots of PA supernatant induced changes in the levels of oxygenated phosphatidylethanolamines (PEs) [$\log_2$ (fold change)] versus significance [$-\log_{10}$ (P value)] by *t*-test in co-culture (epithelial + macrophages) cells vs epithelial cells only. Red, blue, and gray circles represent PE oxygenated species significantly decreased, increased or unchanged in epithelial/macrophage co-culture respectively. (**E**) Bar chart showing the amounts of various HpETE containing PE species in HBE cells treated with PA supernatant with and without macrophage co-culture. Number on top of bars represent the adjusted p value (FDR) vs HBE + PA Sup., n = 3. . (For interpretation of the references to color in this figure legend, the reader is referred to the Web version of this article.)

lipidomics analysis (Fig. 4C). Indeed, we found a significant decrease in the previously established proferroptotic signals 15-HpETE-PEs in HBE cells co-cultured with macrophages (Fig. 4D and E) [10,12].

3. Discussion

The association of ferroptosis with various disease conditions ranging from neurodegenerative disorders, ischemia-reperfusion injury, organ failure to resistant cancers is now well established [31]. This also prompted a search for new ferroptosis resistance mechanisms which led to the discovery of ferroptosis suppressor protein-1 (FSP1) [21,22] and inducible nitric oxide synthase (iNOS) [23]. Overexpression of FSP1 rescues ferroptosis through NAD(P)H/FSP1/CoQ10 axis, independently of GPx4 [21,22]. Similarly, activation of iNOS in M1 macrophages or microglia confers resistance to ferroptosis by preventing lipid peroxidation [23].

In this study, we attempted to investigate the role of host NO• as an intercellular anti-ferroptotic mechanism against PA induced ferroptosis. We demonstrate that after activation, macrophage generated NO• disseminates to surrounding epithelial cells, where it disrupts pathogen triggered ferroptotic process, and protects epithelial cells from ferroptotic death. This unique intercellular anti-ferroptotic function of NO• is due to its small size, lipophilic and highly diffusible nature and its ability to prevent lipid peroxidation, including enzymatic peroxidation catalyzed by 15LOXes: pLoxA in PA supernatants and 15LOX/PEBP1 complexes in mammalian cells [23,44].

For the host, GPx4/GSH anti-oxidant system is the central shield against lipid hydroperoxide driven ferroptotic cell death and is emerging as a prime target for pathogens to chase and exploit for their benefit [10,18,45]. Even though the breakdown of this shield is sufficient to trigger ferroptosis, our previous work and the results of this study suggest that *P. aeruginosa* targets multiple host pathways. On the one hand, *P. aeruginosa* secreted lipoxygenase hijacks host lipid modelling pathway to generate pro-ferroptotic signals and, on the other hand, the pathogen manipulates the host defense system responsible for eliminating such signals (Fig. 1) [10]. Similarly, in tuberculosis, *Mycobacterium tuberculosis* induced ferroptosis is considered to be one of the primary mechanisms of infection and is postulated as a promising target for therapeutic intervention [18]. Hence, assuming ferroptosis a part of the virulence repertoire of PA, we have uncovered an important protective (anti--ferroptotic) role for host NO•. This is important for two main reasons i) host epithelial cells are defenseless and overtaken by the pathogen; ii) the pathogen utilizes outer membrane vesicles (OMV) as a primary source of virulence executioners which interact and alter the host biology without any need for an actual direct contact [32–34].

As GPx4 is a central armor for the cell against formation of lipid hydroperoxides [12,20,46], its degradation is a mandatory signaling event in the execution of ferroptotic cell death [12,20]. Similar to classical ferroptosis inducers like erastin or RSL3, PA supernatant induces degradation of GPx4 leading to intensified lipid hydroperoxide generation and ferroptosis (Fig. 1) [10]. Recently, the mechanisms leading to depletion of GPx4 has attracted a lot of attention and a hope that it will give us additional tools to control, study and understand ferroptotic cell death pathway [46]. The mechanisms are emerging but still are not completely clear. Two independent studies have demonstrated the involvement of lysosomal protein degradation pathway in erastin induced GPx4 degradation-one through activation of Lamp2a [47] and the other one via acid sphingomyelinase (ASM) mediated redox amplification [48]. In this study, we demonstrate that treatment of PA supernatant leads to Lamp2a mediated GPx4 depletion through CMA activation. The presence of lysosomal degradation inhibitors (NH_4Cl and CQ), resulted in diminished PA induced lipid peroxidation and restoration of GPx4 protein levels.

NO• is a potent signaling molecule with the ability to act in a paracrine manner during smooth muscle relaxation or vascular dilation or act as intracellular secondary messenger regulating anti-oxidant response [25,44]. Inducible nitric oxide synthase (iNOS) generated NO• - through interactions with superoxide radicals to produce peroxynitrite, is considered as the first line of host immune defense response against invading pathogens particularly the intracellular ones [25,26,49]. In addition, NO•'s ability to interact with different radicals, including lipid radical intermediates during ferroptosis, can facilitate post-translational nitrosylation of proteins modifying their activity, stability or localization [27]. We found that expression of iNOS did not stabilize or prevent degradation of GPx4, but prevented generation of lipid hydroperoxides and ferroptosis even under GPx4 insufficient conditions. This highlights the role of iNOS/NO• as GPx4 independent regulator of ferroptosis. The fact that NO• is protective against different types of ferroptosis inducers (RSL3, erastin or PA) and is competent locally as well as remotely far away from the source of its generation makes it an important anti-ferroptotic regulatory factor. These features of NO• may have crucial implications in tumors or in chronic *P. aeruginosa* or *M. tuberculosis* lung infections, where the neighboring microenvironment influences the outcome of the target cells. It has been reported that in epithelial cancer cells, E-cadherin mediated intercellular signaling via E-cadherin-NF2-Hippo-YAP axis enhances the resistance to ferroptosis of all cells involved [50]. It is well known that normally low abundance of *P. aeruginosa*, may be substantially elevated in conditions leading to the immune-compromised states such as massive irradiation of cancer patients [51,52]. It is possible that employment of NO•- donors may represent a promising therapeutic strategy in these patients as well in cases of exposure to total body irradiation after accidental or intentional catastrophic circumstances [53].

Lipid peroxidation is one of hallmarks of ferroptosis [12,43,54]. In biological systems, lipid peroxidation can proceed via enzymatic or non-enzymatic mechanisms [55]. While free ionic iron or complexes of iron with low molecular weight ligands represent major non-enzymatic catalysts of free radical lipid peroxidation, lipoxygenases, cyclooxygenases, and cytochromes P450 are the major enzymes involved in lipid peroxidation [14,55]. Under normal conditions, these enzymes predominantly utilize *free* polyunsaturated fatty acids as their substrates of oxygenation reactions yielding different lipid mediators, mostly regulating inflammatory responses [56,57]. 15LOXs can also catalyze peroxidation of polyunsaturated fatty acid residues of phospholipids [16]. Ferroptosis is marked by accumulation of unstable

hydroperoxy-phospholipids and subsequent failure of GSH/GPX4 system to reduce them to the respective alcohols. While both non-enzymatic and enzymatic pathways may be involved in ferroptosis, the selectivity and specificity of characteristic products, hydroperoxy-phosphatidylethanolamines, suggests the involvement of enzymatic pathways in the initiation of the process [58]. Our data demonstrate that irrespective of the source of $NO^{\bullet}$, either from overexpression in HBE cells or from neighboring macrophages, it decreases lipid peroxidation and prevents epithelial ferroptosis induced not only by PA but also by other inducers. In addition, in the co-culture system we observed that the epithelial cells generate a significantly lower amount of pro-ferroptotic 15-HpETE-PE signals. This protection from different types of ferroptotic cell death inducers suggests a general anti-ferroptotic regulatory role of $NO^{\bullet}$. Inhibition of lipid peroxidation by nitric oxide may be realized via several mechanisms [59,60]. Among them are the reduction of the catalytic 15LOX iron, scavenging of lipid radical intermediates during peroxidation and competitive inhibition by $NO^{\bullet}$ of molecular oxygen delivery through specialized channels in the complex of 15LOX with a scaffold-protein, PEBP1, catalyzing peroxidation of polyunsaturated phosphatidylethanolamines (Unpublished results) [60,61]. While all three modes of action can participate in the inhibition of ferroptosis, further detailed studies are needed to quantitatively assess their specific contribution.

Overall, this study highlights a new intercellular anti-ferroptotic role of $NO^{\bullet}$ with immense implications in the context of host-pathogen interaction. The anti-ferroptotic function of $NO^{\bullet}$ is fueled by its small size, diffusible nature and ability to react with enzymatic machinery generating hydroperoxy-PE as well as with radical intermediates of pro-ferroptotic signals. Importantly, iNOS/$NO^{\bullet}$ functions independently of GPx4, protecting GPx4 deficient cells from ferroptosis. Furthermore iNOS/$NO^{\bullet}$ system is equally competent against different ferroptosis inducers (PA supernatant, RSL3, erastin), thus providing another universal layer of protection against ferroptotic death of the host epithelium.

4. Materials and methods

4.1. Reagents

MEM (Thermo Fisher Scientific, 11095-080), FCS (Gibco, 10437-028), Lysogeny broth (LB) (Sigma-Aldrich, L3152), RSL3 (Selleck Chemicals, S8155), erastin (Selleck Chemicals, S7242), ferrostatin-1 (Sigma-Aldrich, SML0583), Chloroquine (Sigma, C6628), NH4Cl (Sigma, A9434), MG132 (Selleck Chemicals, S2619), P3421 (Selleck Chemicals, S1013), 1400W (Cayman, 81520), L-NIL (Cayman, 80310), BSA (Sigma-Aldrich), DETA-NONOate and DPTA-NONOate (Caymen Chemical), NADPH (Sigma), Glutathione peroxidase (Sigma G6137), Cumene hydroperoxide (Sigma C0524), Thiol fluorescent probe IV (Millipore 595504), Glutathione reductase (Sigma), Glutathione reduced (Sigma G4251), 15-HpETE-PE (Caymen Chemical), Pierce BCA Protein Assay Kit (Thermo Fisher Scientific, 23225), anti- GPx4 (rabbit monoclonal, Abcam, ab125066), anti-Lamp2a (Abcam, ab18528), anti-iNOS (Abcam, ab3523), anti-actin (mouse monoclonal, Sigma-Aldrich, A3854, clone AC-15), secondary antibody, goat anti-rabbit (Sigma-Aldrich, A0545).

4.2. Cell culture

Macrophages (RAW 264.7) from ATCC were cultured at 37 °C and 5% CO_2 in DMEM (ATCC) supplemented with 10% fetal calf serum (FCS; Sigma-Aldrich) and 100 U ml^{-1} penicillin– streptomycin (ThermoFisher Scientific). HBE (bronchial epithelial cell line originally established by D. Gruenert) was maintained in minimum essential medium (MEM; ThermoFisher) supplemented with 10% FCS (Gibco), 50 U ml^{-1} penicillin–streptomycin (ThermoFisher), plasmocin (InvivoGen) and L-glutamine (ThermoFisher) as described previously [10,23,62]. HT-1080 cells from ATCC were cultured in EMEM media (ATCC) containing 10% fetal calf serum (FCS; Sigma-Aldrich) and 100 U ml^{-1} penicillin–streptomycin (ThermoFisher Scientific) and incubated at 37 °C and 5% CO_2.

4.3. Bacterial strains

The *P. aeruginosa* hyper-biofilm mutant (*Δwsp*F) and the pLoxA deficient (*loxA::Tn*) strains used in this study was obtained from the *P. aeruginosa* transposon mutant library, University of Washington (Seattle), as described previously [10]. *P. aeruginosa* respiratory isolates (Tobramycin-resistant) from ICUs were identified at the clinical microbiology laboratory of University of Pittsburgh Medical Center (IRB no. PRO12060302) and designated TRPA002–TRPA122 as described previously [10].

4.4. PA supernatant collection

P. aeruginosa was grown in LB medium at 37 °C, 220 r.p.m for 14 h and then re-inoculated in MEM medium (without phenol red) at an OD600 of 0.05 in 96-well vinyl microtitre plates (100 μl per well; Costar). Plates were then incubated at 37 °C without agitation for 24 h. Supernatant was collected by centrifugation (2X) at 3,000 g for 8 min and then frozen before further use in cell culture experiments [10].

4.5. siRNA knockdown experiments

Two Dicer-substrate si-RNAs against iNOS (mm.Ri. Nos2.13.1 and mm.Ri. Nos2.13.2) or GPx4 (hs.Ri.GPX4.13.1 and hs.Ri.GPX4.13.2) or control scrambled DsiRNA (51-01-14-04) (Integrated DNA Technology) were transfected into macrophages or epithelial cells (HBE) using RNAimax (Life Technology) according to the manufacturer's instructions. After transfection (12 h or 8 h), cells were counted and seeded into a 6-well plate for co-culture experiments or 6 cm dishes for western blotting, and treated with PA supernatant for 48 h.

4.6. Overexpression of iNOS

Epithelial or HT-1080 cells were transfected with 1 μg of vector only (pCMV6) or pCMV6-iNOS DNA using Lipofectamine 3000 (Life Technology) for 12 h. Cells were then counted and seeded for cell death or Lipid ROS experiments in the absence or presence of Fer-1 or iNOS inhibitors (L-NIL and 1400W) as indicated. Epithelial cells were transfected with 1 μg of vector only (pCMV6) or pCMV6-GPx4 DNA using Lipofectamine 3000 (Life Technology) for 12 h. Cells were then counted and seeded for Lipid ROS experiments.

4.7. GPx4 activity

HT-1080 untreated and PA supernatant treated cell pellet was resuspended in 0.1 M Tris (pH 8.0) and 150 mM NaCl containing protease/phosphatase inhibitor (1X) and sonicated (3X, 10s on 15s off, at 20%). After sonication, cell lysate was centrifuged at 12000 rpm for 14 min and the supernatant was collected and estimated for protein concentration using BCA kit. Reaction was performed using 120 μg of protein in buffer containing 0.1 M Tris (pH8.0), 1.25% triton X-100 along with 50 μM of HpETE-PE, glutathione (3 mM), glutathione reductase (1 U ml^{-1}) and NADPH (120 μM). Consumption of NADPH was measured by fluorescence using Shimadzu spectrofluorimeter RF-5301 PC. Fluorescence measurements were performed in a 50 μl quartz cuvette using an excitation wavelength of 340 nm, emission wavelength 460 nm (excitation and emission slits of 5 nm and 3 nm, respectively).

4.8. Ferroptosis assay

Epithelial cells were seeded in 24-well plates (20,000 cells per well) for 48 h and then treated with PA Sup. or RSL3 or erastin along with

ferrostatin 1 or protein degradation inhibitors MG132, PS341, NH4Cl and Chloroquine (CQ) or NO - donors for 20 h. Cell death was monitored by PI staining using flow cytometry as described previously [10]. For macrophages, cells were plated in 24 well plates and then activated with PA supernatant for 24 h. Then cells were incubated in fresh media along with RSL3 or erastin and cell death estimated after 12 h by LDH release assay as previously reported [12,23]. HT-1080 untreated or pCMV6 or iNOS expressing cells (20,000 per well) after seeding in 24 well plate for 24 h were treated with PA supernatant with Fer.1 or NO – donors for 20 h. Cell death was monitored by PI staining using flow cytometry as described previously [10].

4.9. Lipid ROS analysis by BODIPY-C11

To analyze lipid ROS, epithelial cells were seeded in 12 well plates for 48 h before treating with PA supernatant. After 14 h of treatment, cells were incubated with 5 μM BODIPY 581/592-C11 (Invitrogen, D3861) for 25–30 min at 37 °C. Cells were then trypsinized, washed with HBSS (2X) and resuspended in HBSS followed by flow cytometric analysis using FL1 channel in BD Canto-II flow cytometer (BD Biosciences). For data analysis FlowJo software was used.

4.10. Co-culture experiments

Epithelial cells 0.08×10^6 per well were seeded in 6well plates for 48 h and then labeled with CellTracker Green (Invitrogen, C7025) (5 μM) for 45 min as previously described. After washing (3X) with PBS, macrophages (0.08×10^6) were added and incubated for 6 h before treating the co-cultured cells with PA supernatant along with Fer.1 or iNOS inhibitor L-NIL. Cells were trypsinized and labeled with fixable Zombie NIR viability kit (BioLegend, 423105) as per the instructions of the manufacturer. Briefly, after washing with PBS, cells were incubated in 100 μl Zombie NIR in PBS (1:1000 diluted) for 30 min in the dark and then washed with PBS containing 0.1% BSA. Finally, cells were fixed with 4% paraformaldehyde and analyzed by flow cytometry. Acquisition was performed by multicolor flow cytometry using LSRII cytometer with FACS DIVA software (BD Bioscience). Double positive (Cell tracker $Green^+/Zombie^+$) epithelial cells were considered for analysis using FlowJo software.

4.11. Western blot analysis

Cell lysates were prepared after washing cells with PBS and lysing in buffer (25 mM Tris-HCl, pH 7.5, 150 mM NaCl and 1% SDS) or by resuspending the pellet in RIPA buffer (ThermoFisher) containing freshly added protease-phosphatase cocktail inhibitor mix (ThermoFisher). Samples were sonicated and total protein amount was estimated by bicinchoninic acid (BCA) protein assay (ThermoFisher) and diluted in 2x Laemmli buffer before loading in 8–16% Tris-glycine gradient gels (Life Technologies). Subsequently, proteins were transferred to PVDF membrane and blocked with PBST (5% milk) for 1 h and the proteins were detected using anti-GPX4 (1:2000), anti-iNOS (1:1000), anti-Lamp2a (1:1000) and anti-βactin (1:1000 for 1 h), antibodies following overnight incubation at room temperature. Membranes were washed with PBST (3X) and then incubated with HRP-conjugating goat anti-rabbit (1:2000 1 h) and then developed with SuperSignal West Pico Chemiluminescent Substrate (ThermoFisher) using Amersham Imager 600 (GE Health Care, Life Sciences).

To determine expression of iNOS protein in macrophages by flow cytometry, cells were stained with anti-CD11b antibody conjugated with BUV605 (Biolegend) followed by the intracellular staining with fixation and permeabilization using anti-iNOS antibody conjugated with AlexaFL700 (BD Bioscience).

4.12. GSH measurements

GSH measurements were performed as described previously [10]. Briefly, cells were resuspended in 50 μl of PBS and then lysed by freeze-thaw and bath sonication. Samples 10 μl in triplicate were incubated with 10 μM Thiol fluorescent probe IV (Millipore) for 5 min and then analyzed with an excitation and emission wavelength of 400 nm and 465 nm using the Cytation 5 imaging reader (BioTek). GSH amount was normalized by protein concentration measured by BCA method. To estimate the contribution of other small molecular weight thiols, we utilized untreated (control) and erastin treated HBE cells and pre-incubated the samples with Glutathione peroxidase from bovine erythocytes and cumene hydroperoxide to selectively oxidize GSH. After this, we added the excess of a thiol fluorescent probe (10 μM). We found that the contribution of other small thiols was minor and did not exceed 10% of the response in the presence of endogenous GSH (Supplementary Fig. 3).

For GSH/GSSG measurement, the sample was treated with 2 U mL^{-1} of glutathione reductase (Sigma) and 30 μM of NADPH (Sigma Aldrich) at room temperature for 30 min to reduce all present GSSG to GSH. After reaction, untreated and reduced sample was taken in duplicate at 10 μl amounts and incubated with 10 μM Thiol Fluorescent Probe IV (Millipore) at room temperature for 5 min and analyzed with an excitation and emission wavelength of 400 nm and 465 nm using the Cytation 5 Imaging Reader (BioTek). Thiol Fluorescent Probe IV contains reactivity toward 2-ME, GSH, and cysteine but not non-thiol-containing GSSG or cystine. Therefore, the GSSG amount was calculated by taking the GSH difference of reduced and untreated samples and divided by two (1 GSSG yields 2 GSH). GSH amounts were normalized by protein concentration measured by BCA method.

4.13. Determination of pLoxA activity in P. aeruginosa clinical isolates

Supernatant from clinical isolates (50 μl) was mixed with 50 μl of 20 mM HEPES buffer, pH 7.4, containing 100 μM DTPA, 10 μM AA (arachidonic acid), and 0.5 μM 15-HOO-AA-PE and incubated for 10 min at 37 °C. Then samples were extracted by Folch procedure [12,16] and analyzed by LC-MS. Data were normalized to the amount of protein and presented as AAoxidation (pmol/min/μg of protein).

4.14. LC–MS analysis of phospholipids

MS analysis of phospholipids was performed on an Orbitrap Fusion Lumos mass spectrometer (ThermoFisher). Phospholipids were separated on a normal phase column (Luna 3 μm Silica (2) 100 Å, 150 × 2.0 mm, Phenomenex) at a flow rate of 0.2 ml min^{-1} on a Dionex Ultimate 3000 HPLC system. The column was maintained at 35 °C. Analysis was performed using gradient solvents (A and B) containing 10 mM ammonium acetate. Solvent A contained propanol:hexane:water (285:215:5, vol/vol/vol) and solvent B contained propanol:hexane: water (285:215:40, vol/vol/vol). All solvents were LC–MS grade. The column was eluted for 0–23 min with a linear gradient of 10–32% B; 23–32 min using a linear gradient of 32–65% B; 32–35 min with a linear gradient of 65–100% B; 35–62 min held at 100% B; 62–64 min with a linear gradient from 100% to 10% B followed by and equilibration from 64 to 80 min at 10% B. The instrument was operated with the electrospray ionization probe in negative polarity mode. Analysis of LC–MS data was performed using software package Compound Discoverer (ThermoFisher) with an in-house generated analysis workflow and oxidized phospholipid database. Lipids were further filtered by retention time and confirmed by fragmentation mass spectrum.

4.15. Partial correlation analysis

Partial correlation analysis was performed using the function pcor.test from ppcor package in R languages. Partial correlation analysis was

performed between ferroptotic cell death and GSH or pLoxA while controlling for pLoxA or GSH levels respectively. Residual scatter plot was plotted using ggplot2 package of R language.

4.16. Statistical analysis

The data in figure legends are presented as mean ± s.d. values from at least three experiments unless otherwise specified. In general, the exact value of sample size (n) is presented in the figure legends and reflects either the number of experimental replications with cells or biochemical model systems. Statistical analyses were performed by One-way ANNOVA, Tukeys multiple comparisons test, unless otherwise specified.

Author contributions

H. H. D., H. B and V. E. K conceived the study. H. H. D., L. A. P. and A. B. S. performed all cell experiments. T. S. A. performed lipidomics experiments and analyzed the data and performed correlation analysis. H. H. D., A. B. S. and G. V. S. performed flow experiments and analyzed data. A. O. K. performed GSH measurements and analyzed the data. V. A. T performed pLoxA activity experiments and LC-MS analysis. J. S. L. participated in selection and testing of clinical isolates. R. K. M. and S. E. W. participated in formulating the idea and interpreted the results. J.S. L. and H. B. participated in writing the manuscript. H. H. D and V. E. K wrote the manuscript. All authors read and approved the final manuscript.

Declaration of competing interest

The authors declare no conflicting interest.

Acknowledgements

This work was supported by the NIH grants numbers: HL114453, AI156924, AI156923, CA165065, CA243142, AI145406, NS076511, NS061817 (V.E.K and H.B); National Heart, Lung, And Blood Institute of the National Institutes of Health under Award Numbers R01 HL136143, P01 HL114453 (J S.L).

Appendix A. Supplementary data

Supplementary data to this article can be found online at https://doi.org/10.1016/j.redox.2021.102045.

References

[1] M.R. Rogan, L.L. Patterson, J.Y. Wang, J.W. McBride, Bacterial manipulation of wnt signaling: a host-pathogen tug-of-wnt, Front. Immunol. 10 (2019).
[2] R.T. Sadikot, T.S. Blackwell, J.W. Christman, A.S. Prince, Pathogen-host interactions in Pseudomonas aeruginosa pneumonia, Am. J. Respir. Crit. Care Med. 171 (2005) 1209–1223.
[3] K. Labbé, M. Saleh, Cell death in the host response to infection, Cell Death Differ. 15 (2008) 1339–1349.
[4] D.R. Green, The coming decade of cell death research: five riddles, Cell 177 (2019) 1094–1107.
[5] I. Jorgensen, M. Rayamajhi, E.A. Miao, Programmed cell death as a defence against infection, Nat. Rev. Immunol. 17 (2017) 151–164.
[6] D. Tang, R. Kang, T.V. Berghe, P. Vandenabeele, G. Kroemer, The molecular machinery of regulated cell death, Cell Res. 29 (2019) 347–364.
[7] H. Ashida, H. Mimuro, M. Ogawa, T. Kobayashi, T. Sanada, M. Kim, C. Sasakawa, Cell death and infection: a double-edged sword for host and pathogen survival, J. Cell Biol. 195 (2011) 931–942.
[8] S.M. Behar, M. Divangahi, H.G. Remold, Evasion of innate immunity by Mycobacterium tuberculosis: is death an exit strategy? Nat. Rev. Microbiol. 8 (2010) 668–674.
[9] L. Böhme, T. Rudel, Host cell death machinery as a target for bacterial pathogens, Microb. Infect. 11 (2009) 1063–1070.
[10] H.H. Dar, Y.Y. Tyurina, K. Mikulska-Ruminska, I. Shrivastava, H.-C. Ting, V. A. Tyurin, J. Krieger, C.M. St Croix, S. Watkins, E. Bayir, et al., Pseudomonas aeruginosa utilizes host polyunsaturated phosphatidylethanolamines to trigger theft-ferroptosis in bronchial epithelium, J. Clin. Invest. 128 (2018) 4639–4653.
[11] S. Doll, M. Conrad, Iron and ferroptosis: a still ill-defined liaison, IUBMB Life 69 (2017) 423–434.
[12] V.E. Kagan, G. Mao, F. Qu, J.P. Angeli, S. Doll, C.S. Croix, H.H. Dar, B. Liu, V. A. Tyurin, V.B. Ritov, et al., Oxidized arachidonic and adrenic PEs navigate cells to ferroptosis, Nat. Chem. Biol. 13 (2017) 81–90.
[13] B.R. Stockwell, J.P. Friedmann Angeli, H. Bayir, A.I. Bush, M. Conrad, S.J. Dixon, S. Fulda, S. Gascón, S.K. Hatzios, V.E. Kagan, et al., Ferroptosis: a regulated cell death nexus linking metabolism, redox biology, and disease, Cell 171 (2017) 273–285.
[14] D.A. Stoyanovsky, Y.Y. Tyurina, I. Shrivastava, I. Bahar, V.A. Tyurin, O. Protchenko, S. Jadhav, S.B. Bolevich, A.V. Kozlov, Y.A. Vladimirov, et al., Iron catalysis of lipid peroxidation in ferroptosis: regulated enzymatic or random free radical reaction? Free Radic. Biol. Med. 133 (2019) 153–161.
[15] T.S. Anthonymuthu, Y.Y. Tyurina, W.Y. Sun, K. Mikulska-Ruminska, I. H. Shrivastava, V.A. Tyurin, F.B. Cinemre, H.H. Dar, A.P. VanDemark, T. R. Holman, et al., Resolving the paradox of ferroptotic cell death: ferrostatin-1 binds to 15LOX/PEBP1 complex, suppresses generation of peroxidized ETE-PE, and protects against ferroptosis, Redox Biol 38 (2021) 101744.
[16] S.E. Wenzel, Y.Y. Tyurina, J. Zhao, C.M. St Croix, H.H. Dar, G. Mao, V.A. Tyurin, T. S. Anthonymuthu, A.A. Kapralov, A.A. Amoscato, et al., PEBP1 wardens ferroptosis by enabling lipoxygenase generation of lipid death signals, Cell 171 (2017) 628–641, e626.
[17] J. Zhao, V.B. O'Donnell, S. Balzar, C.M. St Croix, J.B. Trudeau, S.E. Wenzel, 15-Lipoxygenase 1 interacts with phosphatidylethanolamine-binding protein to regulate MAPK signaling in human airway epithelial cells, Proc. Natl. Acad. Sci. U. S. A. 108 (2011) 14246–14251.
[18] E.P. Amaral, D.L. Costa, S. Namasivayam, N. Riteau, O. Kamenyeva, L. Mittereder, K.D. Mayer- Barber, B.B. Andrade, A. Sher, A major role for ferroptosis in Mycobacterium tuberculosis-induced cell death and tissue necrosis, J. Exp. Med. 216 (2019) 556–570.
[19] J.P. Friedmann Angeli, M. Schneider, B. Proneth, Y.Y. Tyurina, V.A. Tyurin, V. J. Hammond, N. Herbach, M. Aichler, A. Walch, E. Eggenhofer, et al., Inactivation of the ferroptosis regulator Gpx4 triggers acute renal failure in mice, Nat. Cell Biol. 16 (2014) 1180–1191.
[20] W.S. Yang, R. SriRamaratnam, M.E. Welsch, K. Shimada, R. Skouta, V. S. Viswanathan, J.H. Cheah, P.A. Clemons, A.F. Shamji, C.B. Clish, et al., Regulation of ferroptotic cancer cell death by GPX4, Cell 156 (2014) 317–331.
[21] K. Bersuker, J.M. Hendricks, Z. Li, L. Magtanong, B. Ford, P.H. Tang, M.A. Roberts, B. Tong, T.J. Maimone, R. Zoncu, et al., The CoQ oxidoreductase FSP1 acts parallel to GPX4 to inhibit ferroptosis, Nature 575 (2019) 688–692.
[22] S. Doll, F.P. Freitas, R. Shah, M. Aldrovandi, M.C. da Silva, I. Ingold, A. Goya Grocin, T.N. Xavier da Silva, E. Panzilius, C.H. Scheel, et al., FSP1 is a glutathione-independent ferroptosis suppressor, Nature 575 (2019) 693–698.
[23] A.A. Kapralov, Q. Yang, H.H. Dar, Y.Y. Tyurina, T.S. Anthonymuthu, R. Kim, C. M. St Croix, K. Mikulska-Ruminska, B. Liu, I.H. Shrivastava, et al., Redox lipid reprogramming commands susceptibility of macrophages and microglia to ferroptotic death, Nat. Chem. Biol. 16 (2020) 278–290.
[24] V.A.N. Kraft, C.T. Bezjian, S. Pfeiffer, L. Ringelstetter, C. Müller, F. Zandkarimi, J. Merl-Pham, X. Bao, N. Anastasov, J. Kössl, et al., GTP cyclohydrolase 1/ tetrahydrobiopterin counteract ferroptosis through lipid remodeling, ACS Cent. Sci. 6 (2020) 41–53.
[25] F. Aktan, iNOS-mediated nitric oxide production and its regulation, Life Sci. 75 (2004) 639–653.
[26] D.O. Schairer, J.S. Chouake, J.D. Nosanchuk, A.J. Friedman, The potential of nitric oxide releasing therapies as antimicrobial agents, Virulence 3 (2012) 271–279.
[27] A.J. Gow, Q. Chen, D.T. Hess, B.J. Day, H. Ischiropoulos, J.S. Stamler, Basal and stimulated protein S-nitrosylation in multiple cell types and tissues, J. Biol. Chem. 277 (2002) 9637–9640.
[28] R. Radi, Oxygen radicals, nitric oxide, and peroxynitrite: redox pathways in molecular medicine, Proc. Natl. Acad. Sci. U. S. A. 115 (2018) 5839–5848.
[29] J. MacMicking, Q.W. Xie, C. Nathan, Nitric oxide and macrophage function, Annu. Rev. Immunol. 15 (1997) 323–350.
[30] A. Linkermann, R. Skouta, N. Himmerkus, S.R. Mulay, C. Dewitz, F. De Zen, A. Prokai, G. Zuchtriegel, F. Krombach, P.-S. Welz, et al., Synchronized renal tubular cell death involves ferroptosis, Proc. Natl. Acad. Sci. U.S.A. 111 (2014) 16836–16841.
[31] B.R. Stockwell, X. Jiang, W. Gu, Emerging mechanisms and disease relevance of ferroptosis, Trends Cell Biol. 30 (2020) 478–490.
[32] J.M. Bomberger, D.P. Maceachran, B.A. Coutermarsh, S. Ye, G.A. O'Toole, B. A. Stanton, Long-distance delivery of bacterial virulence factors by Pseudomonas aeruginosa outer membrane vesicles, PLoS Pathog. 5 (2009), e1000382.
[33] C. Schwechheimer, M.J. Kuehn, Outer-membrane vesicles from Gram-negative bacteria: biogenesis and functions, Nat. Rev. Microbiol. 13 (2015) 605–619.
[34] J. Vitse, B. Devreese, The contribution of membrane vesicles to bacterial pathogenicity in cystic fibrosis infections and healthcare associated pneumonia, Front. Microbiol. 11 (2020) 630.
[35] M.M. Gaschler, A.A. Andia, H. Liu, J.M. Csuka, B. Hurlocker, C.A. Vaiana, D. W. Heindel, D.S. Zuckerman, P.H. Bos, E. Reznik, et al., FINO(2) initiates ferroptosis through GPX4 inactivation and iron oxidation, Nat. Chem. Biol. 14 (2018) 507–515.
[36] J.M. Bomberger, K.H. Ely, N. Bangia, S. Ye, K.A. Green, W.R. Green, R.I. Enelow, B. A. Stanton, Pseudomonas aeruginosa Cif protein enhances the ubiquitination and proteasomal degradation of the transporter associated with antigen processing (TAP) and reduces major histocompatibility complex (MHC) class I antigen presentation, J. Biol. Chem. 289 (2014) 152–162.

[37] A.M. Cuervo, J.F. Dice, A receptor for the selective uptake and degradation of proteins by lysosomes, Science 273 (1996) 501–503.
[38] S. Kaushik, A.M. Cuervo, Chaperone-mediated autophagy: a unique way to enter the lysosome world, Trends Cell Biol. 22 (2012) 407–417.
[39] J. Dächert, H. Schoeneberger, K. Rohde, S. Fulda, RSL3 and Erastin differentially regulate redox signaling to promote Smac mimetic-induced cell death, Oncotarget 7 (2016) 63779–63792.
[40] J. Zheng, M. Conrad, The metabolic underpinnings of ferroptosis, Cell Metabol. 32 (2020) 920–937.
[41] Scott J. Dixon, Kathryn M. Lemberg, Michael R. Lamprecht, R. Skouta, Eleina M. Zaitsev, Caroline E. Gleason, Darpan N. Patel, Andras J. Bauer, Alexandra M. Cantley, Wan S. Yang, et al., Ferroptosis: an iron-dependent form of nonapoptotic cell death, Cell 149 (2012) 1060–1072.
[42] L.E. Donnelly, P.J. Barnes, Expression and regulation of inducible nitric oxide synthase from human primary airway epithelial cells, Am. J. Respir. Cell Mol. Biol. 26 (2002) 144–151.
[43] W.S. Yang, B.R. Stockwell, Ferroptosis: death by lipid peroxidation, Trends Cell Biol. 26 (2016) 165–176.
[44] R. Korhonen, A. Lahti, H. Kankaanranta, E. Moilanen, Nitric oxide production and signaling in inflammation, Curr. Drug Targets - Inflamm. Allergy 4 (2005) 471–479.
[45] M. Matsushita, S. Freigang, C. Schneider, M. Conrad, G.W. Bornkamm, M. Kopf, T cell lipid peroxidation induces ferroptosis and prevents immunity to infection, J. Exp. Med. 212 (2015) 555–568.
[46] T.M. Seibt, B. Proneth, M. Conrad, Role of GPX4 in ferroptosis and its pharmacological implication, Free Radic. Biol. Med. 133 (2019) 144–152.
[47] Z. Wu, Y. Geng, X. Lu, Y. Shi, G. Wu, M. Zhang, B. Shan, H. Pan, J. Yuan, Chaperone-mediated autophagy is involved in the execution of ferroptosis, Proc. Natl. Acad. Sci. U.S.A. 116 (2019) 2996–3005.
[48] F. Thayyullathil, A.R. Cheratta, A. Alakkal, K. Subburayan, S. Pallichankandy, Y. A. Hannun, S. Galadari, Acid sphingomyelinase-dependent autophagic degradation of GPX4 is critical for the execution of ferroptosis, Cell Death Dis. 12 (2021) 26.
[49] D. Chakravortty, M. Hensel, Inducible nitric oxide synthase and control of intracellular bacterial pathogens, Microb. Infect. 5 (2003) 621–627.
[50] J. Wu, A.M. Minikes, M. Gao, H. Bian, Y. Li, B.R. Stockwell, Z.-N. Chen, X. Jiang, Intercellular interaction dictates cancer cell ferroptosis via NF2–YAP signalling, Nature 572 (2019) 402–406.
[51] S. Gerassy-Vainberg, A. Blatt, Y. Danin-Poleg, K. Gershovich, E. Sabo, A. Nevelsky, S. Daniel, A. Dahan, O. Ziv, R. Dheer, et al., Radiation induces proinflammatory dysbiosis: transmission of inflammatory susceptibility by host cytokine induction, Gut 67 (2018) 97–107.
[52] O. Zaborina, J.E. Kohler, Y. Wang, C. Bethel, O. Shevchenko, L. Wu, J.R. Turner, J. C. Alverdy, Identification of multi-drug resistant Pseudomonas aeruginosa clinical isolates that are highly disruptive to the intestinal epithelial barrier, Ann. Clin. Microbiol. Antimicrob. 5 (2006), 14-14.
[53] S. Garg, M. Boerma, J. Wang, Q. Fu, D.S. Loose, K.S. Kumar, M. Hauer-Jensen, Influence of sublethal total-body irradiation on immune cell populations in the intestinal mucosa, Radiat. Res. 173 (2010) 469–478.
[54] M. Conrad, V.E. Kagan, H. Bayir, G.C. Pagnussat, B. Head, M.G. Traber, B. R. Stockwell, Regulation of lipid peroxidation and ferroptosis in diverse species, Genes Dev. 32 (2018) 602–619.
[55] E. Niki, Y. Yoshida, Y. Saito, N. Noguchi, Lipid peroxidation: mechanisms, inhibition, and biological effects, Biochem. Biophys. Res. Commun. 338 (2005) 668–676.
[56] R.A. Siddiqui, K. Harvey, W. Stillwell, Anticancer properties of oxidation products of docosahexaenoic acid, Chem. Phys. Lipids 153 (2008) 47–56.
[57] A. Umeno, V. Biju, Y. Yoshida, In vivo ROS production and use of oxidative stress-derived biomarkers to detect the onset of diseases such as Alzheimer's disease, Parkinson's disease, and diabetes, Free Radic. Res. 51 (2017) 413–427.
[58] R. Shah, M.S. Shchepinov, D.A. Pratt, Resolving the role of lipoxygenases in the initiation and execution of ferroptosis, ACS Cent. Sci. 4 (2018) 387–396.
[59] S.G. Hummel, A.J. Fischer, S.M. Martin, F.Q. Schafer, G.R. Buettner, Nitric oxide as a cellular antioxidant: a little goes a long way, Free Radic. Biol. Med. 40 (2006) 501–506.
[60] A.C. Nicolescu, J.N. Reynolds, L.R. Barclay, G.R. Thatcher, Organic nitrites and NO: inhibition of lipid peroxidation and radical reactions, Chem. Res. Toxicol. 17 (2004) 185–196.
[61] Q. Li, C. Li, H.K. Mahtani, J. Du, A.R. Patel, J.R. Lancaster Jr., Nitrosothiol formation and protection against Fenton chemistry by nitric oxide-induced dinitrosyliron complex formation from anoxia-initiated cellular chelatable iron increase, J. Biol. Chem. 289 (2014) 19917–19927.
[62] D.C. Gruenert, M. Willems, J.J. Cassiman, R.A. Frizzell, Established cell lines used in cystic fibrosis research, J. Cyst. Fibros. 3 (Suppl 2) (2004) 191–196.